

Published in final edited form as:

Nature. 2015 April 30; 520(7549): 670–674. doi:10.1038/nature14125.

An Epigenome-Wide Association Study of Total Serum Immunoglobulin E Concentration

Liming Liang¹, Saffron A.G. Willis-Owen^{#2}, Catherine Laprise^{#3}, Kenny C.C. Wong², Gwyneth A. Davies⁴, Thomas J. Hudson^{5,6}, Aristeia Binia², Julian M. Hopkin⁴, Ivana V. Yang⁷, Elin Grundberg⁸, Stephan Busche⁸, Marie Hudson⁹, Lars Rönnblom¹⁰, Tomi M. Pastinen^{8,11}, David A. Schwartz⁷, G. Mark Lathrop^{8,*}, Miriam F. Moffatt^{2,*}, and William O.C.M. Cookson^{2,*}

¹Departments of Epidemiology and Biostatistics, Harvard School of Public Health, Boston, MA 02115

²National Heart and Lung Institute, Imperial College, London SW3 6LY, UK

³Université du Québec à Chicoutimi, Saguenay, Québec, Canada

⁴Institute of Life Science, College of Medicine, Swansea University, SA2 8PP, UK

⁵Ontario Institute for Cancer Research, Toronto, Ontario Canada, M5G 0A3

⁶Departments of Medical Biophysics and Molecular Genetics, University of Toronto, Canada ON M5S 1A1

⁷University of Colorado School of Medicine and National Jewish Health, Denver, CO 80206

⁸Department of Human Genetics, McGill University and Génome Québec Innovation Centre, Montréal, Canada

⁹Jewish General Hospital and Lady Davis Research Institute, Montréal, Canada H3T 1E2

¹⁰Department of Medical Sciences, SciLifeLab, Uppsala University, Uppsala, Sweden

¹¹Department of Medical Genetics, McGill University Health Centre, Montréal, Canada

These authors contributed equally to this work.

Abstract

Users may view, print, copy, and download text and data-mine the content in such documents, for the purposes of academic research, subject always to the full Conditions of use:http://www.nature.com/authors/editorial_policies/license.html#terms

Address for Correspondence: Professor William O. C. Cookson, Imperial College London, Royal Brompton Campus, Guy Scadding Building, Dovehouse Street, London SW3 6LY, Phone: +44 20 7594 2943, w.cookson@imperial.ac.uk.

Author contributions: SWO, WOCC, GML and MFM planned the initial study. SWO, AB, KCW and MFM performed measurements of methylation status. LL and WOCC led statistical analyses of the data with SWO and GML: most analyses were carried out by LL. GML and TMP led discussions on replication strategy, methylation assays and cell-specific methylation, with input from MFM, DS and IY. EG validated Illumina probes with bisulphite sequencing. CL led studies of SLSJ families with TH, and GD and JMH led studies of the PAPA subjects. CL led studies of isolated eosinophils. MH, LR and SB recruited subjects and studied lymphocyte subsets. WOCC wrote the first draft of the paper. All authors contributed to the interpretation of the results and the writing of the paper.

*Contributed equally.

The authors declare no competing financial interests.

Immunoglobulin E (IgE) is a central mediator of allergic (atopic) inflammation. Therapies directed against IgE benefit hay fever¹ and allergic asthma^{1,2}. Genetic association studies have not yet identified novel therapeutic targets or pathways underlying IgE regulation³⁻⁶. We therefore surveyed epigenetic association between serum IgE concentrations and methylation at loci concentrated in CpG islands (CGI) genome-wide in 95 nuclear pedigrees, using DNA from peripheral blood leukocytes (PBL). We validated positive results in additional families and in subjects from the general population. We show here replicated associations with a meta-analysis false discovery rate $<10^{-4}$ between IgE and low methylation at 36 loci. Genes annotated to these loci encode known eosinophil products, and also implicate phospholipid inflammatory mediators, specific transcription factors, and mitochondrial proteins. We confirmed that methylation at these loci differed significantly in isolated eosinophils from subjects with and without high IgE levels. The top three loci accounted for 13% of IgE variation in the primary subject panel, explaining 10 fold higher variance than that derived from large SNP GWAS^{3,4}. The study identifies novel therapeutic targets and biomarkers for patient stratification for allergic diseases.

Asthma, atopic dermatitis (eczema) and hay fever are IgE-related diseases that are increasing in prevalence and are a major source of disability. Systematic knowledge of IgE production is limited, beyond the regulation of IgE creation in B-cells by Interleukin-4 (IL4) released from T_H2 cells and eosinophils⁷. Genome-wide association studies show polymorphisms in *STAT6*, *FCERIA*, *IL4/RAD50* and the MHC to be associated with high IgE concentrations³⁻⁶, but these SNPs combined account for only 1-2% of the variation in serum IgE⁴.

CpG methylation is associated with gene silencing and the patterning of gene expression that determines cellular types and functions⁸, and islands of CpG (CGI) sequences are positioned near the promoters of 40% of human genes⁹. *IL4* expression has been related to upstream epigenetic variation in DNA methylation in T-cells¹⁰, encouraging us to search genome-wide for other CGI associated with IgE serum concentrations.

We used Illumina HumanMethylation27 arrays to target individual CpG sites (loci) within proximal promoter regions of 14,475 genes. The panel is enriched for genomic regions regulating expression, but does not cover all functionally important CpG sites. We excluded from downstream analyses any loci with SNPs overlapping the Illumina probe sequence, and established that direct bisulphite pyrosequencing correlates robustly with the array in our hands (Extended Data Figure 1) and elsewhere¹¹.

We investigated nuclear families from the MRCA panel in which we have previously carried out genome-wide SNP association studies for IgE levels and asthma¹². The panel contained 355 subjects (183 male) with a mean age in children of 12.2 years (ranging from 2 to 39) and adults of 42 years (27 to 61) (Table 1). 113 children had doctor-diagnosed asthma (DDAST). We sought for replication in 149 Caucasian subjects selected equally from the top and bottom deciles of IgE distribution in 1,614 unselected volunteers for the PAPA study (Poplogaeth Asthma Prifysgol Abertawe: students and staff from Swansea University)¹³; and in 160 subjects in an asthmatic family panel from the Saguenay–Lac-Saint-Jean region (SLSJ) of Quebec¹⁴ with a mean age in children of 16 years (ranging from 5 to 50; 40 DDAST) and adults of 44 years (31 to 79)(Table 1).

We fitted models with Ln(IgE) as dependent variable and methylation status for each Illumina probe as a predictor with age, sex, parental status, interactions and batch identifiers as covariates. We identified 34 loci with a false discovery rate (FDR) <0.01 (Figure 1 and Supplementary Table 1) in 32 different CGIs in the MRCA panel. Following replication in PAPA and SLSJ panels a meta-analysis combining the results identified 36 loci with FDR $<10^{-4}$ and 62 loci with an FDR <0.005 (Table 2 and Supplementary Table 1). All loci showed associations with the same anti-correlated direction in the three datasets (Table 2). A RAST index, quantifying IgE against common allergens¹⁵, showed similar but non-independent associations, suggesting common regulation of total and specific IgE. Testing of models with asthma as the dependent variable showed only *LPCAT2* and *ZNF22* to be associated with asthma independently of IgE levels ($P=7.7\times 10^{-5}$ and $P=1.8\times 10^{-4}$).

The variable methylation site upstream of *IL4* has a well-studied effect on *IL4* production^{16,17} and IgE regulation, with methylation anticorrelated with expression in the same direction as in our study. We looked for SNP associations at this locus by imputation with the 1000G phase 1 SNPs and indels in all three panels, analysing the 20,746 variants within 1Mb upstream or downstream of the *IL4* 5'UTR. We found no significant SNP associations with IgE after accounting for multiple testing.

We carried out Mendelian randomization to test for a causal effect of *IL4* methylation on IgE¹⁸, choosing the SNP showing strongest association to methylation at the *IL4* CpG probe (cg26787239) as the instrumental variable. The First Stage F-test statistics for the MRCA and SLSJ panels ($F=16.4$ and 26.2) indicated effects strong enough to ensure the validity of the method. In the MRCA panel, association between the instrument SNP (*rs12311504*) and IgE before adjusting for *IL4* methylation was $P=0.03$ and $P=0.53$ after adjustment, indicating that methylation mediated most of the SNP effect. The meta-analysis P for a causal effect was 6.8×10^{-4} , suggesting that the locus represents a functionally validated epigenetic association with a complex phenotype.

Several loci were annotated to genes that encode proteins characteristic of eosinophils (Table 2 and Supplementary Table 1). *IL5RA* encodes a receptor that selectively stimulates eosinophil production and activation¹⁹; *CCR3* encodes the eosinophil eotaxin receptor; *IL1RL1* encodes the receptor for the eosinophil-activating cytokine IL33; *PGR2* encodes eosinophil granule major basic protein (*PRG2*); *PGR3* is a *PGR2* homologue; and *GATA1* is an eosinophil transcription factor. We therefore tested whether methylation at our associated loci marked activation in eosinophils purified from peripheral blood, studying 8 asthmatics with high serum IgE levels (>110 IU/L), 8 asthmatics with low serum IgE (<110 IU/L) levels and 8 controls (mean age all subjects 31 years (range 6-56), 8 females and 2 current smokers). Asthmatics in both groups were on a maintenance regime of inhaled beta agonists, augmented with inhaled glucocorticoids during exacerbations.

We observed the lowest levels of methylation in the subjects with asthma and high IgE and that methylation in asthmatics with low IgE was intermediate to controls (Figure 2) ($P<0.05$; Supplementary Table 1), supporting our initial results. Partitioning the data into high or low IgE groups gave similar conclusions. The range of variation for the principal loci was narrower in asthmatics with high IgE (Figure 2) than in the other two groups, suggesting the

enrichment of a distinctive eosinophil subset in atopic asthma. This is consistent with the recognised mixture of eosinophil populations in human blood and eosinophil activation in atopic disease²⁰. Comparison of methylation levels in the MRCA panel for our IgE-associated loci ($P < 0.001$) with an independent study of eosinophils isolated from normal subjects²¹ confirmed correlations with methylation status ($R = 0.64$).

Lineage commitment to particular cell types is accompanied by specific methylation changes⁸, and it has been suggested that DNA from mixtures of cells (such as PBL) will not support EWAS of complex diseases²¹. We extracted DNA from unfractionated populations of PBL, so that our methylation patterns reflect the numbers and the activity of different cells in each specimen. We further explored whether our associations to IgE reflected carriage in particular cell types by fitting regression models that included differential white cell counts. We identified partial associations with eosinophil numbers for all IgE associated loci (Supplementary Table 2 and Figure 3), consistent with independent effects on IgE from the numbers of eosinophils and the activity of the loci within eosinophils.

It is well recognised that the regulation of IgE production against particular antigens may reside in T-cells and B-cells as well as in eosinophils²². Our regression models however found that the top IgE associations were not accounted for by concomitant correlation with lymphocyte counts (Supplementary Table 2). We further examined the distribution of our IgE-associated CpG loci in leukocyte subsets isolated in our Centre and in subsets from published data²¹. The results showed robustly in both datasets that low levels of methylation at the IgE associated loci were confined to eosinophils (Extended Data Figure 2).

Surrogate CpG markers that identify lymphocyte subsets can be used as an alternative to white cell counts in association models²³. We also applied these methods to our data (Extended Data Table 1). This analysis provided further evidence that T-cell subsets do not have strong effects on these loci.

The variance (Standard Deviation) in our IgE-associated CpG loci was on average 4.4 fold larger in isolated eosinophils than in PBL from the MRCA dataset, indicating an attenuation of effect size in PBL that would mask associations rather magnify them. The power to detect cell-specific associations from PBL depends on the proportion of each cell type, the effect size in specific cells, and the sample size. We estimated that we had 90% power to detect loci accounting for 10% of variance in IgE in the MRCA panel and >99% power in the combined panels (Extended Data Figure 3). Although our ability to detect associations was enhanced by eosinophil counts that were above the normal range for many of our subjects (Table 1), the power estimates and the large observed effect size encourage EWAS of other diseases in which PBLs may be important.

We investigated the variance attributable to different loci in the MRCA panel through a stepwise regression that included all significant CGI associations together with differential white cell counts, age, sex and parental status. Using a cut-off of corrected $P < 0.1$ for inclusion, we found *SLC25A33*, *LPCAT2* and *L2HGDH* to predict the serum IgE concentration independently of each other and of eosinophil counts.

In the MRCA panel the top 3 CpGs independently explained 13.5% IgE variation and counts 8.8%, and in the SLSJ panel the top 3 CpGs explained 8.3% IgE variation and counts 15.5%. (We were not able to estimate variances meaningfully in the PAPA dataset, because the samples were selected by extreme IgE values). The regression models therefore matched the results from isolated eosinophils, with the conclusion the methylation status of eosinophils and their numbers were both related to IgE levels.

Methylation levels were highly correlated between loci and similar estimations of variance were obtained with forced entry of other significantly associated markers, so the results do not imply that *SLC25A33*, *LPCAT2* and *L2HGDH* are the most important loci. DNA methylation is not meiotically heritable and the variance in IgE attributable to these loci does not impact on the problem of missing heritability.

Overall, the most significant association was to *cg01998785*, within a CGI adjacent to *LPCAT2* (also known as *AYTL1*). *LPCAT2* encodes lyso-platelet-activating factor (PAF) acetyltransferase, which is essential to induced formation of PAF, a potent pro-inflammatory lipid mediator²⁴. It is of interest that hypoactive variants of plasmatic PAF-acetylhydrolase are associated with atopy and asthma²⁵. Other significant associations annotated to genes involved in phospholipid metabolism included lysoplasmalogenase (*TMEM86B*), *CEL* and *CLC*.

GATA1 is a known eosinophil transcription factor and subsequent investigations will determine if the other associated transcription factors *ZNF22*, *RBI* and *KLF* regulate eosinophil activation. Other associations may encode proteins released from eosinophil granules, including *PRG2*, *PRG3*, *SERPINC1* (antithrombin), *TFF1* (which may protect the mucosa), *CEL* (carboxyl ester lipase), and the polyvalent serine protease inhibitor *SPINK4*. Genes encoding mitochondrial proteins (*L2HGDH* and *SLC25A3*) are consistent with mitochondrial suppression of apoptosis in activated eosinophils²⁶.

Although the relationship between methylation and gene expression at these loci requires further investigation in isolated cells, our results support the recognition that eosinophils are an important source of cytokines and other pro-inflammatory molecules at the site of allergic inflammation⁷. Eosinophils are required locally for the maintenance of bone-marrow plasma cells²⁷, allowing direct regulation of IgE production in specialised environments. Clinically, the presence of eosinophilia in the peripheral blood or airways identifies a subgroup of refractory asthmatic individuals in whom therapies directed at eosinophils may be effective²⁸. The measurement of methylation at these loci may identify patients responsive to therapies directed at eosinophils or individual gene products.

Cigarette smoking may increase serum IgE, and we found anti-correlated associations to current cigarette smoking with *F2RL3* ($P=8.6\times 10^{-17}$) and *GPR15* ($P=4.6\times 10^{-9}$). The SLSJ dataset confirmed these associations ($P=2.5\times 10^{-6}$ and $P=6.6\times 10^{-7}$), in keeping with previous studies^{29,30}. Adjusting for smoking had minimal impact on the top hits for IgE and neither locus affected IgE in our subjects. *F2RL3* and *GPR15* may represent therapeutic targets to counter tobacco smoke and their methylation status may prospectively predict consequences of smoking.

Our EWAS has discovered reproducible CGI associations accounting for a variation in the total serum IgE that is 10 fold higher than that derived from large SNP GWAS⁴. In contrast to SNP studies, association to methylation levels captures responses to environmental factors and the loci should not be assumed to cause disease. Nevertheless, our findings suggest the presence of novel therapeutically tractable pathways underlying IgE production.

Online Methods

Phenotyping

Ethical approval for the study was obtained from the NHS Multicentre Research Ethics Committee for the MRCA subjects; from the Swansea Joint Scientific Research Committee and Swansea Research Ethics Committee for the Swansea (PAPA) subjects; and from le Centre de Santé et des Services Sociaux de Chicoutimi for the SLSJ families. Written informed consent was obtained from all subjects or in the case of children, from their parents. Asthma was doctor defined. Following a standard respiratory questionnaire, all subjects submitted to venipuncture. Differential white cell counts were measured by automated counter. Total serum IgE and specific serum IgE to whole HDM (*Dermatophagoides pteronyssinus*) and Timothy grass pollen (*Phleum pratense*) were measured using the Immunocap FEIA (Pharmacia AB, Uppsala, Sweden). The levels of specific IgE were converted to RAST units according to Pharmacia recommendations. A combined RAST index was calculated for each individual as the sum of the RAST scores to HDM and Timothy grass¹⁵.

Detection of Methylation status

DNA was extracted after red cell lysis and centrifugation to recover leukocyte nuclear pellets. DNA samples were bisulfite converted using the Zymo EZ DNA Methylation kit (Zymo Research, Orange, CA, USA) with an input of 1000ng. The assay was carried out as per the Illumina Infinium Methylation instructions, using the HumanMethylation27 BeadChips (Illumina Inc, San Diego, CA, USA). These interrogate 27,578 of CpG sites for the extent of DNA methylation. Data were visualized using the BeadStudio software, and samples that failed quality control were repeated. Raw methylation data was exported from the GenomeStudio software. For the Illumina HumanMethylation27 BeadChip data, quantile normalization of intensity was applied to all methylated and unmethylated probes for all samples together. The methylation β values were recalculated as the ratio of methylated probe signal/(total signal + 100). The Touleimat and Tost³¹ analysis pipeline was used for the HumanMethylation450 BeadChip. Individual data points with detection $P > 0.01$ or number of beads < 3 were treated as missing data, as were samples with more than 20% missing probes. The lumi package³² was used for background and colour bias correction. BeadChip ID and position on chip were included as categorical covariates to account for potential batch effects. Quantile normalization across samples was applied to probes within each functional category (CpG island, shelf, shore, etc.) separately to correct the shift of methylation beta value between Infinium I and Infinium II probes on the HumanMethylation450 BeadChip. Probe overlaps with any frequent SNP (MAF $> 5\%$ in 1000 Genomes Project phase 1 EUR population) in the probe sequence or in position +1 or +2 of the query site (depending on Infinium I or Infinium II status) were removed. The use

of meta-analysis to combine 27K and 450K data together with this implementation of the Tost pipeline ensured our analysis was not confounded by probe differences.

Isolation of human eosinophils

Isolation of human eosinophils was as described³³. Briefly, platelet-rich plasma was removed from 200ml using centrifugation, followed by Dextran-mediated sedimentation to remove erythrocytes and removal of mononuclear cells using a lymphocyte separation medium. Hypotonic lysis with sterile water removed remaining erythrocytes and other granulocytes were removed using negative selection with anti-CD16 MicroBeads. DNA was extracted using the QIAamp® DNA Blood Mini Kit. Methylation was assessed using Illumina 450K arrays, with analysis restricted to significantly associated probes from the meta analysis.

Statistical analyses

In order to investigate the association with the total serum IgE concentration we tested for association with log-normalized IgE ($\text{Ln}(\text{IgE})$) as response with methylation (β) at each locus as predictor whilst including Sex, Age, Parent indicator, Age*Sex and Age*Parent interactions in the model, together with batch indicators captured by Illumina chip ID and position of chip (such as operators, sample wells, plates, runs, and reagents). We applied inverse normal transformation to methylation measures to remove the effect of outliers. We used the R function `lme()` in the `nlme` package to implement a linear mixed model, assuming a compound symmetry variance-covariance structure to account for correlation of phenotypes among family members. The R code for the discovery stage of association in the MRCA panel was:

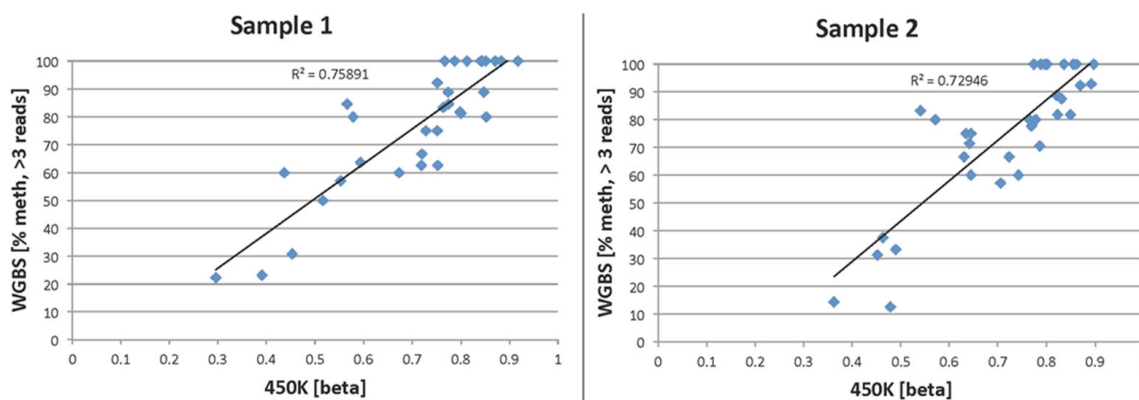
```
index=!is.na(methylation)
fam=familyID[index]
par=parent[index]
methylation = methylation [index]
methylation =qnorm(rank(methylation)/(length(methylation)+1),mean=0,sd=1)
lnige=LNIGE[index]
age=AGE[index]
sex=SEX[index]

lm2=lme(lnige~sex+age+methylation+par+sex*age+age*par,random=~1|fam)
```

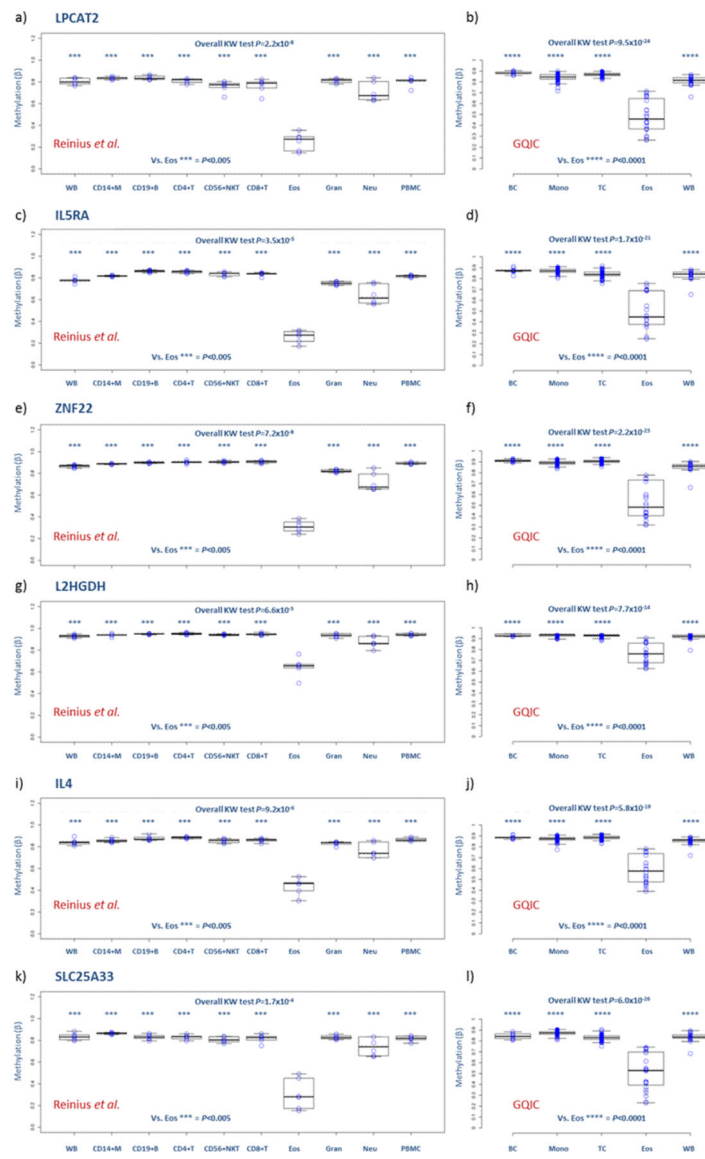
The residual methylation value after removal of effects of chip ID and position for the genome-wide significant loci in the MRCA, PAPA and SLSJ panels is provided in Supplementary Tables 3-5, together with phenotypic and covariate parameters. We calculated false discovery rates (FDR) and applied Bonferroni corrections to adjust for multiple comparisons to 27,578 probes. The same analyses were carried out in the PAPA

and SLSJ subjects before meta-analysis of the three datasets. We use a weighted z-score method for meta-analysis based on pvalue and effect direction from individual studies with weights proportion to the square root of sample size of individual study³⁴. SNPs and indels from the 1000 Genomes Project phase 1 release (2012-03-14 haplotypes) were imputed using MINIMAC³⁵. SNPs or indels with imputation quality score $R^2 < 0.3$ were removed from downstream analysis. We carried out Mendelian randomization to assess the causal effect of IL4 methylation on IgE level through a 2 stage least square instrumental variable regression³⁶ implemented in the ivreg2.r program (<http://diffuseprior.wordpress.com/2012/05/03/an-ivreg2-function-for-r/>). We tested association trends in isolated eosinophils by exact regression (Cytel Studio 9) with asthma/high IgE coded as 2, asthma/low IgE coded as 1, and controls as 0. Covariates for age, sex, and batch were included in the model and to test the hypothesis that low levels of methylation were associated with high IgE, *P* values were one-sided. Differences in methylation between peripheral blood leukocyte subsets were assessed with Kruskal-Wallis tests, using two-sided *P* values.

Extended Data



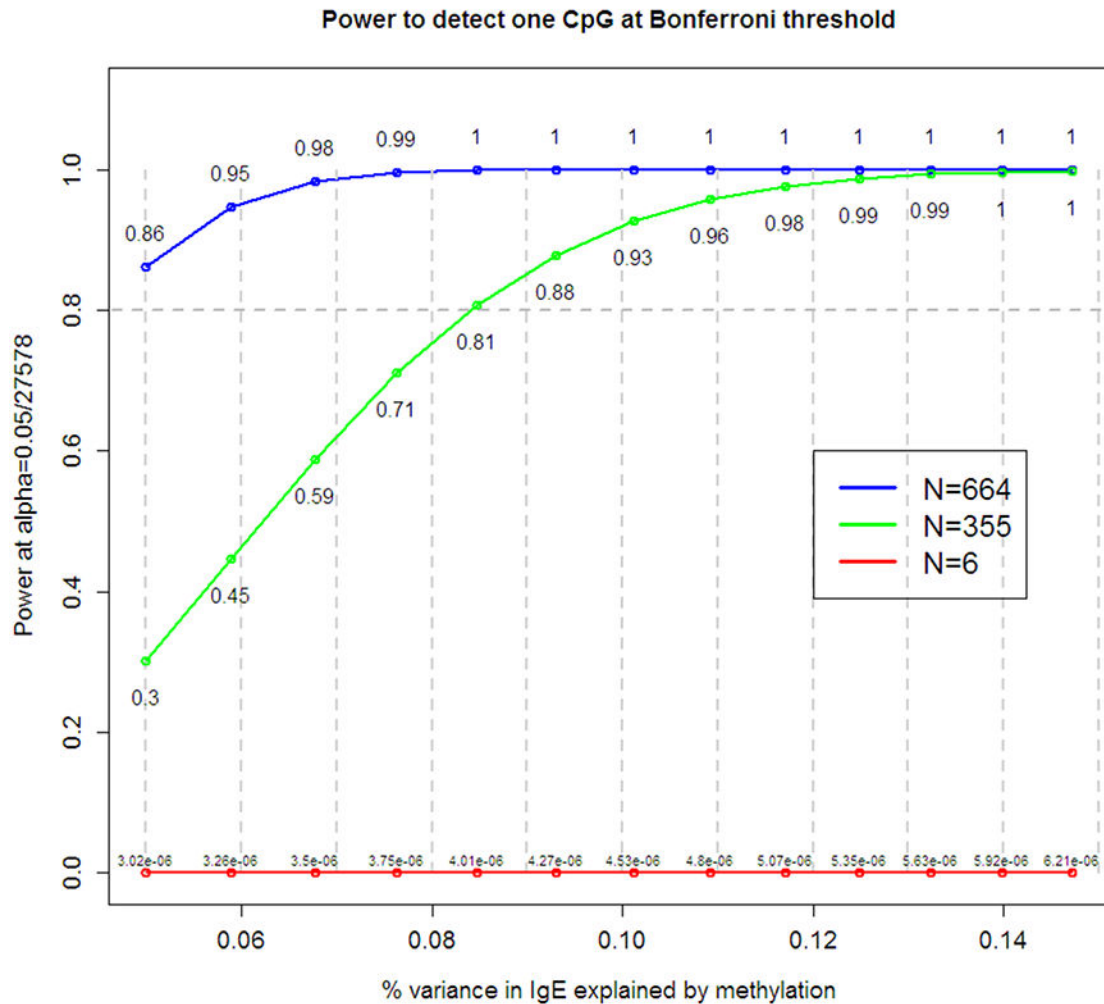
Extended Data Figure 1. Concordance in methylation status at IgE-associated loci when comparing whole-genome bisulphite sequencing (WGBS) with the Illumina platform
 These results were produced by us (EG and TMP) at the Genome Quebec Innovation Centre. The figures show a comparison between IgE-associated CpG probes using Illumina 450K (x-axis) and WGBS (y-axis) platforms for two samples (left and right panels) with 20 fold sequence coverage. The results show a high R^2 between platforms (0.76 and 0.73). The median of the correlation coefficients for our IgE associated loci across 30 different samples (using WGBS at various depths) was $R^2=0.76$. This to be compared with the global assessment of all overlapping 450K sites which is $R^2=0.81$.



Extended Data Figure 2. Distribution of methylation status at IgE-associated loci in isolated leukocyte subsets

The figure shows the distribution of methylation in peripheral blood leukocyte subsets at the most strongly IgE-associated loci. CpG methylation was measured by the Illumina Infinium 450K platform. Boxplots show means and interquartile ranges. **a, c, e, g, i, k**) Results from publically available data derived from 6 healthy controls (Reinius *et al*²¹). Lower levels of methylation with wider variation is observed in eosinophils when compared to whole blood (WB) and subsets comprising CD14+ Monocytes (CD14+M); CD19+ B cells (CD19+B); CD4+ T-cells (CD4+T); CD56+ natural killer cells (CD56+NK); CD8+ T cells (CD8+T); granulocytes (Gran); Neutrophils (Neu) and PBMC. **b, d, f, h, j, l**) Results from cells isolated and analyzed by us at the Genome Quebec Innovation Centre (GQIC). Eosinophils (Eos) (from 24 subjects in the SLSJ panel) also show lower levels of methylation with wider variation compared to whole blood (WB, 22 SLSJ subjects), and to subsets including B-cells

(BC, 9 control subjects), Monocytes (Mono, 76 control subjects), and T-cells (TC, 74 control subjects).



Extended Data Figure 3. Power estimations to detect eosinophil-specific effects in DNA from peripheral blood lymphocytes

The figure shows that our original MRCA dataset (green line) and our combined dataset (blue line) are well powered to detect signals of the magnitude observed in our three groups of subjects. The red line shows the power of sample size of 6 described in Reinius *et al.*²¹ to detect differences in CpG methylation in unfractionated PBL. The mean variance (as standard deviation, SD) for the IgE-associated loci was 0.036 in PBLs from our primary MRCA panel and 0.023 in the whole blood normal samples from Reinius *et al.*²¹, demonstrating that our results were consistent with the previous experiment.

Extended Data Table 1 Comparison of surrogate variable analyses with direct white cell counts in association models

The table shows the I values from regression models in the MRCA panel that predict lnIgE at each locus a) before adjusting cell counts; b) after adjusting cell counts using Houseman surrogate variables; c) after adjusting for cell subsets counted in our data. pMethyl measures strength of association to IgE. CD8, CD4 and NK are Tcell subsets, GRAN= granulocytes, EOS=eosinophils, NEU=neutrophil, LYM=lymphocytes, MON=monocytes, BAS=basophils. All models are adjusted for sex, age, methylation, parent/child status, sex*age interaction, and age*parent interaction.

Chr.	Position	Symbol	a) Before adjusting cell counts										b) Adjusting for Houseman cell proportions										c) Adjusting for white cell counts									
			probe	pMethy	pCD8T	pMethy	pCD4T	pNK	pBCELL	pMON	pGRAN	pMethy	pEOS	pNEU	pLYM	pMON	pBAS															
1	9521654	SLC25A33	cg18783781	4.96E-14	5.58E-13	0.3625663	0.6489145	0.0830001	0.0735391	0.7715233	0.2564499	6.14E-06	0.00065	0.866661	0.678896	0.561016	0.551752															
16	54100210	LPCAT2	cg01998785	1.24E-13	3.81E-13	0.1560292	0.3633042	0.034881	0.0300831	0.7239839	0.1881862	2.36E-06	0.0003	0.294806	0.300248	0.445243	0.785135															
14	49849865	L2HGDH	cg15996947	7.39E-13	3.81E-11	0.3709841	0.6823007	0.125117	0.1583239	0.9387673	0.3768824	3.21E-05	0.000295	0.38062	0.519495	0.662394	0.890493															
10	44815441	ZNF22	cg01614759	4.42E-12	9.09E-11	0.3526504	0.6420391	0.1382946	0.0810812	0.654088	0.3845248	7.61E-05	0.000216	0.305013	0.42021	0.601202	0.937252															
3	3127530	IL5RA	cg10159529	5.06E-12	1.70E-10	0.8786628	0.9388517	0.2941882	0.2701973	0.9752202	0.5129874	0.000104	6.81E-05	0.877227	0.802458	0.551635	0.756105															
1	172153108	SERPINC1	cg01770400	6.59E-12	1.54E-11	0.1182883	0.3063038	0.0323251	0.0368702	0.574556	0.1896	6.56E-06	0.000109	0.236406	0.186757	0.667289	0.90807															
21	42659768	TFF1	cg02643667	7.87E-12	6.81E-11	0.234861	0.4646176	0.0330799	0.0706689	0.797703	0.1753888	9.07E-06	0.384611	0.725574	0.672431	0.976409																
5	132036424	IL4	cg26787239	1.59E-11	2.13E-10	0.5058003	0.9922092	0.1723318	0.1996409	0.7364825	0.6544331	1.25E-05	0.269226	0.259295	0.614387	0.77939																
2	110014086	LIMS3	cg18879041	4.06E-11	2.57E-09	0.3708111	0.7030526	0.1613161	0.2166898	0.9745824	0.474026	0.000865	0.000256	0.280498	0.382954	0.500203	0.963467															
13	47774920	RB1	cg13221796	5.66E-10	9.26E-11	0.1278218	0.3641314	0.0353766	0.0458363	0.7786051	0.2987933	2.84E-06	1.83E-05	0.029037	0.081617	0.516731	0.982861															
19	60432000	TMEM86B	cg26457013	1.02E-09	4.08E-09	0.3305229	0.5920938	0.036091	0.0792481	0.9078355	0.2711535	0.000691	1.35E-05	0.363948	0.317448	0.538421	0.740734															
9	100745613	COL15A1	cg20503329	1.19E-09	3.14E-08	0.4772819	0.7388277	0.1359031	0.1343368	0.9433195	0.4284566	0.001341	1.17E-05	0.443838	0.49736	0.401174	0.959364															
1	31166502	SDC3	cg07689731	2.33E-09	4.79E-09	0.5074834	0.7985815	0.0774502	0.0726484	0.7924958	0.4108301	0.002906	1.48E-05	0.415182	0.483806	0.437372	0.932638															
21	45317773	ADARB1	cg09676390	1.21E-08	1.32E-07	0.43369	0.6702876	0.0791369	0.1103603	0.9234331	0.3292778	0.000472	3.48E-07	0.432091	0.530921	0.462608	0.820656															
9	134926722	CEL	cg03693099	1.84E-08	1.01E-07	0.2926779	0.512945	0.0818301	0.1071869	0.9754856	0.3848947	0.000383	9.27E-06	0.099207	0.18224	0.575481	0.93957															
19	12859426	KLFI	cg26136776	3.34E-08	5.42E-07	0.2328607	0.4764967	0.0498737	0.087521	0.7661611	0.2312155	0.008494	4.25E-06	0.308908	0.378613	0.526765	0.764392															
X	48529968	GATA1	cg00536175	7.85E-08	5.70E-07	0.6056632	0.9159691	0.163687	0.1102612	0.8082841	0.5675393	0.002444	1.31E-06	0.230592	0.333849	0.423511	0.745501															
12	10222881	TMEM52B	cg25494227	1.29E-07	2.79E-07	0.4810187	0.6746518	0.0457622	0.0735827	0.9017706	0.3386288	8.31E-05	2.05E-08	0.349366	0.362883	0.456694	0.75634															
9	33229641	SPINK4	cg00079056	1.54E-07	1.23E-06	0.3893041	0.6595419	0.067607	0.090288	0.950103	0.3262354	0.015058	9.70E-07	0.327361	0.481372	0.49343	0.779557															
12	15017287	PDE6H	cg09447105	2.16E-07	1.80E-06	0.6038815	0.9752817	0.1325361	0.2619219	0.6725442	0.6818338	0.002327	6.73E-07	0.185319	0.308805	0.650588	0.72691															
16	4778723	FLJ25410	cg05215575	3.11E-07	7.40E-08	0.6354446	0.6693211	0.0382164	0.0635217	0.8705757	0.2084314	0.011151	9.08E-08	0.699883	0.891282	0.341595	0.856081															
7	142369547	KEL	cg17784922	4.24E-07	9.07E-07	0.6926023	0.9854571	0.0699431	0.1577229	0.8028496	0.5052827	0.001391	3.21E-08	0.505128	0.698535	0.367309	0.99912															
7	29199993	CHN2	cg21472642	6.51E-07	7.39E-07	0.5225896	0.8312874	0.0708089	0.0764603	0.9022296	0.4725488	8.45E-06	3.38E-09	0.104506	0.231601	0.595919	0.815002															
2	191009029	FLJ20160	cg15998761	9.33E-07	9.09E-06	0.4236314	0.824669	0.1393183	0.1145142	0.8527446	0.4643437	0.043732	5.71E-07	0.331558	0.449501	0.418024	0.785659															
6	25862169	SLC17A4	cg21627181	1.14E-06	1.42E-06	0.7663137	0.9149808	0.0591244	0.1414494	0.9511792	0.3972344	0.025202	5.30E-08	0.609342	0.865393	0.467443	0.746032															
14	49849874	L2HGDH	cg20189937	1.32E-06	1.16E-05	0.503935	0.9204654	0.0921306	0.1950088	0.8817908	0.5174749	0.007269	1.26E-07	0.297519	0.525586	0.480584	0.958405															

Chr.	Position	Symbol	a) Before adjusting cell counts										b) Adjusting for Houseman cell proportions										c) Adjusting for white cell counts									
			probe	pMethy	pMethy	pCD8T	pCD4T	pNK	pBCELL	pMON	pGRAN	pMethy	pEOS	pNEU	pLYM	pMON	pBAS	probe	pMethy	pMethy	pCD8T	pCD4T	pNK	pBCELL	pMON	pGRAN	pMethy	pEOS	pNEU	pLYM	pMON	pBAS
17	39822093	ITGA2B	cg17749520	1.37E-06	9.24E-06	0.3677214	0.6752543	0.046072	0.1157269	0.8717913	0.3274826	0.009625	3.11E-07	0.286277	0.406727	0.666483	0.903996	cg17749520	1.37E-06	9.24E-06	0.3677214	0.6752543	0.046072	0.1157269	0.8717913	0.3274826	0.009625	3.11E-07	0.286277	0.406727	0.666483	
17	39701014	SLC4A1	cg03580247	1.51E-06	1.76E-05	0.4966594	0.7030166	0.1566437	0.1201467	0.7706213	0.4809553	9.19E-05	7.97E-09	0.262889	0.282218	0.522557	0.944194	cg03580247	1.51E-06	1.76E-05	0.4966594	0.7030166	0.1566437	0.1201467	0.7706213	0.4809553	9.19E-05	7.97E-09	0.262889	0.282218	0.522557	
20	41789039	FAM112A	cg11398517	2.42E-06	2.11E-05	0.431888	0.7316467	0.0506171	0.209415	0.8337169	0.4256838	0.006763	1.86E-07	0.220078	0.444385	0.592602	0.918166	cg11398517	2.42E-06	2.11E-05	0.431888	0.7316467	0.0506171	0.209415	0.8337169	0.4256838	0.006763	1.86E-07	0.220078	0.444385	0.592602	
11	56904791	PRG3	cg24459209	3.33E-06	1.29E-05	0.5460024	0.9366639	0.0692143	0.1545826	0.8947187	0.4338765	0.094895	2.69E-07	0.444762	0.621114	0.500854	0.993962	cg24459209	3.33E-06	1.29E-05	0.5460024	0.9366639	0.0692143	0.1545826	0.8947187	0.4338765	0.094895	2.69E-07	0.444762	0.621114	0.500854	
12	7792928	CLEC4C	cg22194129	5.46E-06	0.0001208	0.4977092	0.8378959	0.0710935	0.6019842	0.8886589	0.4447889	0.023532	2.38E-08	0.408481	0.759002	0.521453	0.818552	cg22194129	5.46E-06	0.0001208	0.4977092	0.8378959	0.0710935	0.6019842	0.8886589	0.4447889	0.023532	2.38E-08	0.408481	0.759002	0.521453	
14	95011802	C14orf49	cg16522484	8.04E-06	0.0001668	0.4308412	0.7282314	0.1486239	0.1112817	0.9482318	0.4206034	0.034072	1.01E-07	0.285777	0.449644	0.49125	0.837548	cg16522484	8.04E-06	0.0001668	0.4308412	0.7282314	0.1486239	0.1112817	0.9482318	0.4206034	0.034072	1.01E-07	0.285777	0.449644	0.49125	
X	48529554	GATA1	cg22543648	9.51E-06	7.12E-05	0.682124	0.9511741	0.1312401	0.1917101	0.6997158	0.4748147	0.02664	2.00E-08	0.585973	0.689124	0.425854	0.888172	cg22543648	9.51E-06	7.12E-05	0.682124	0.9511741	0.1312401	0.1917101	0.6997158	0.4748147	0.02664	2.00E-08	0.585973	0.689124	0.425854	
2	11727816	NTSR2	cg25657834	1.02E-05	2.04E-05	0.9354409	0.6331433	0.1373482	0.3261244	0.4920064	0.8015518	5.67E-05	4.84E-10	0.191813	0.526463	0.689339	0.954103	cg25657834	1.02E-05	2.04E-05	0.9354409	0.6331433	0.1373482	0.3261244	0.4920064	0.8015518	5.67E-05	4.84E-10	0.191813	0.526463	0.689339	
19	48912054	IRGC	cg26251865	1.76E-05	9.19E-06	0.714389	0.9562959	0.0555475	0.1095196	0.6922884	0.4367507	0.011533	1.35E-08	0.495745	0.567965	0.468957	0.977824	cg26251865	1.76E-05	9.19E-06	0.714389	0.9562959	0.0555475	0.1095196	0.6922884	0.4367507	0.011533	1.35E-08	0.495745	0.567965	0.468957	
19	44919789	CLC	cg18254848	1.77E-05	2.33E-05	0.7122613	0.874791	0.0834931	0.1954486	0.6341788	0.5277066	0.161753	4.77E-08	0.462599	0.67872	0.424877	0.937408	cg18254848	1.77E-05	2.33E-05	0.7122613	0.874791	0.0834931	0.1954486	0.6341788	0.5277066	0.161753	4.77E-08	0.462599	0.67872	0.424877	
6	10635801	GCNT2	cg26385286	1.78E-05	3.88E-05	0.5747779	0.9758809	0.0654066	0.2046998	0.6574459	0.5308099	0.070861	4.31E-08	0.339931	0.593173	0.451377	0.902264	cg26385286	1.78E-05	3.88E-05	0.5747779	0.9758809	0.0654066	0.2046998	0.6574459	0.5308099	0.070861	4.31E-08	0.339931	0.593173	0.451377	
3	150064527	CPA3	cg13424229	1.89E-05	2.29E-06	0.4329161	0.6962458	0.1048729	0.0674688	0.7084296	0.6214492	0.001236	4.96E-07	0.054043	0.094343	0.451245	0.955257	cg13424229	1.89E-05	2.29E-06	0.4329161	0.6962458	0.1048729	0.0674688	0.7084296	0.6214492	0.001236	4.96E-07	0.054043	0.094343	0.451245	

Supplementary Material

Refer to Web version on PubMed Central for supplementary material.

Acknowledgements

This work was supported by the Freemasons' Grand Charity. The study was also funded by the Wellcome Trust under WT 077959 and WT096964, the UK Medical Research Council, a grant to ML from Génome Québec, le Ministère de l'Enseignement supérieur, de la Recherche, de la Science et de la Technologie (MESRST) Québec and McGill University, and the NIH R01 HL101251-01. M. Moffatt and W. Cookson are Joint Wellcome Trust Senior Investigators, W. Cookson is an NIHR Senior Investigator and C. Laprise is the Chairholder of the Canada Research Chair on Genetic Determinants in Asthma. We thank Anne-Marie Madore and Vanessa T. Vaillancourt for the eosinophil isolation and Michel Laviolette and Nicolas Flamand for their advice on this technique.

References

- Holgate ST, Djukanovic R, Casale T, Bousquet J. Anti-immunoglobulin E treatment with omalizumab in allergic diseases: an update on anti-inflammatory activity and clinical efficacy. *Clin Exp Allergy*. 2005; 35(4):408–416. [PubMed: 15836747]
- Busse WW, et al. Randomized trial of omalizumab (anti-IgE) for asthma in inner-city children. *N Engl J Med*. 2011; 364(11):1005–1015. [PubMed: 21410369]
- Weidinger S, et al. Genome-wide scan on total serum IgE levels identifies FCER1A as novel susceptibility locus. *PLoS Genet*. 2008; 4(8):e1000166. [PubMed: 18846228]
- Moffatt MF, et al. A large-scale, consortium-based genomewide association study of asthma. *N Engl J Med*. 2010; 363(13):1211–1221. [PubMed: 20860503]
- Levin AM, et al. A meta-analysis of genome-wide association studies for serum total IgE in diverse study populations. *J Allergy Clin Immunol*. 2013; 131(4):1176–1184. [PubMed: 23146381]
- Granada M, et al. A genome-wide association study of plasma total IgE concentrations in the Framingham Heart Study. *J Allergy Clin Immunol*. 2012; 129(3):840–845. e821. [PubMed: 22075330]
- Nouri-Aria KT, et al. Cytokine expression during allergen-induced late nasal responses: IL-4 and IL-5 mRNA is expressed early (at 6 h) predominantly by eosinophils. *Clin Exp Allergy*. 2000; 30(12):1709–1716. [PubMed: 11122208]
- Deaton AM, et al. Cell type-specific DNA methylation at intragenic CpG islands in the immune system. *Genome Res*. 2011; 21(7):1074–1086. [PubMed: 21628449]
- Eckhardt F, et al. DNA methylation profiling of human chromosomes 6, 20 and 22. *Nat Genet*. 2006; 38(12):1378–1385. [PubMed: 17072317]
- Lohning M, Richter A, Radbruch A. Cytokine memory of T helper lymphocytes. *Advances in immunology*. 2002; 80:115–181. [PubMed: 12078480]
- Roessler J, et al. Quantitative cross-validation and content analysis of the 450k DNA methylation array from Illumina, Inc. *BMC research notes*. 2012; 5:210. [PubMed: 22546179]
- Moffatt MF, et al. Genetic variants regulating ORMDL3 expression contribute to the risk of childhood asthma. *Nature*. 2007; 448(7152):470–473. [PubMed: 17611496]
- Ziyab AH, et al. Interactive effect of STAT6 and IL13 gene polymorphisms on eczema status: results from a longitudinal and a cross-sectional study. *BMC medical genetics*. 2013; 14:67. [PubMed: 23815671]
- Laprise C. The Saguenay-Lac-Saint-Jean asthma familial collection: the genetics of asthma in a young founder population. *Genes Immun*. 2014
- Palmer LJ, et al. Independent inheritance of serum immunoglobulin E concentrations and airway responsiveness. *Am J Respir Crit Care Med*. 2000; 161(6):1836–1843. [PubMed: 10852754]
- Tykocinski LO, et al. A critical control element for interleukin-4 memory expression in T helper lymphocytes. *J Biol Chem*. 2005; 280(31):28177–28185. [PubMed: 15941711]
- Ansel KM, Djuretic I, Tanasa B, Rao A. Regulation of Th2 differentiation and Il4 locus accessibility. *Annu Rev Immunol*. 2006; 24:607–656. [PubMed: 16551261]

18. Relton CL, Davey Smith G. Two-step epigenetic Mendelian randomization: a strategy for establishing the causal role of epigenetic processes in pathways to disease. *International journal of epidemiology*. 2012; 41(1):161–176. [PubMed: 22422451]
19. Lopez AF, et al. Recombinant human interleukin 5 is a selective activator of human eosinophil function. *The Journal of experimental medicine*. 1988; 167(1):219–224. [PubMed: 2826636]
20. Kita H. Eosinophils: multifaceted biological properties and roles in health and disease. *Immunol Rev*. 2011; 242(1):161–177. [PubMed: 21682744]
21. Reinius LE, et al. Differential DNA methylation in purified human blood cells: implications for cell lineage and studies on disease susceptibility. *PLoS ONE*. 2012; 7(7):e41361. [PubMed: 22848472]
22. Holt PG, Strickland DH, Wikstrom ME, Jahnsen FL. Regulation of immunological homeostasis in the respiratory tract. *Nat Rev Immunol*. 2008; 8(2):142–152. [PubMed: 18204469]
23. Houseman EA, et al. DNA methylation arrays as surrogate measures of cell mixture distribution. *BMC Bioinformatics*. 2012; 13:86. [PubMed: 22568884]
24. Shindou H, et al. A single enzyme catalyzes both platelet-activating factor production and membrane biogenesis of inflammatory cells. Cloning and characterization of acetyl-CoA:LYSO-PAF acetyltransferase. *J Biol Chem*. 2007; 282(9):6532–6539. [PubMed: 17182612]
25. Kruse S, et al. The Ile198Thr and Ala379Val variants of plasmatic PAF-acetylhydrolase impair catalytical activities and are associated with atopy and asthma. *Am J Hum Genet*. 2000; 66(5):1522–1530. [PubMed: 10733466]
26. Peachman KK, Lyles DS, Bass DA. Mitochondria in eosinophils: functional role in apoptosis but not respiration. *Proc Natl Acad Sci U S A*. 2001; 98(4):1717–1722. [PubMed: 11172017]
27. Chu VT, et al. Eosinophils are required for the maintenance of plasma cells in the bone marrow. *Nature immunology*. 2011; 12(2):151–159. [PubMed: 21217761]
28. Pavord ID, et al. Mepolizumab for severe eosinophilic asthma (DREAM): a multicentre, double-blind, placebo-controlled trial. *Lancet*. 2012; 380(9842):651–659. [PubMed: 22901886]
29. Breitling LP, Yang R, Korn B, Burwinkel B, Brenner H. Tobacco-smoking-related differential DNA methylation: 27K discovery and replication. *Am J Hum Genet*. 2011; 88(4):450–457. [PubMed: 21457905]
30. Wan ES, et al. Cigarette smoking behaviors and time since quitting are associated with differential DNA methylation across the human genome. *Hum Mol Genet*. 2012; 21:3073–3082. [PubMed: 22492999]
31. Touleimat N, Tost J. Complete pipeline for Infinium((R)) Human Methylation 450K BeadChip data processing using subset quantile normalization for accurate DNA methylation estimation. *Epigenomics*. 2012; 4(3):325–341. [PubMed: 22690668]
32. Du P, Kibbe WA, Lin SM. lumi: a pipeline for processing Illumina microarray. *Bioinformatics*. 2008; 24(13):1547–1548. [PubMed: 18467348]
33. Ferland C, et al. Eotaxin promotes eosinophil transmigration via the activation of the plasminogen-plasmin system. *J Leukoc Biol*. 2001; 69(5):772–778. [PubMed: 11358986]
34. Willer CJ, Li Y, Abecasis GR. METAL: fast and efficient meta-analysis of genomewide association scans. *Bioinformatics*. 2010; 26(17):2190–2191. [PubMed: 20616382]
35. Howie B, Fuchsberger C, Stephens M, Marchini J, Abecasis GR. Fast and accurate genotype imputation in genome-wide association studies through pre-phasing. *Nat Genet*. 2012; 44(8):955–959. [PubMed: 22820512]
36. Lawlor DA, Harbord RM, Sterne JA, Timpson N, Davey Smith G. Mendelian randomization: using genes as instruments for making causal inferences in epidemiology. *Stat Med*. 2008; 27(8):1133–1163. [PubMed: 17886233]

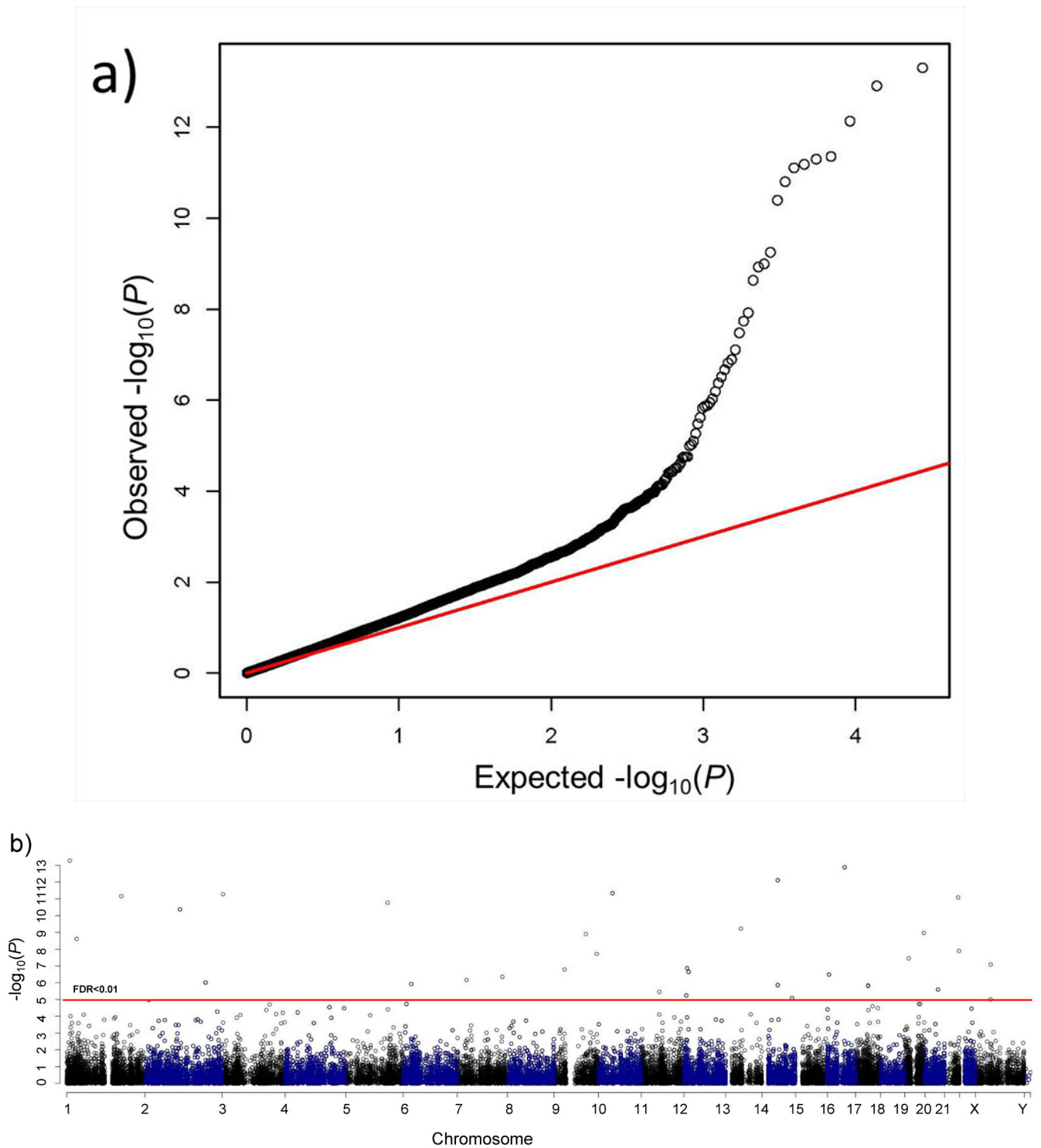


Figure 1. Manhattan plot of the results of the genome-wide methylation association study
 The results of genome-wide association testing to CGI are shown for 27,000 loci in 355 subjects from the MRCA panel of families. **a)** The QQ plot showing observed vs. expected $-\log_{10}P$ values for association at all loci. **b)** Manhattan plot showing chromosomal locations

of $-\log_{10}P$ values for association at each locus. The red line illustrates the threshold for a False Discovery Rate (FDR) <0.01 .

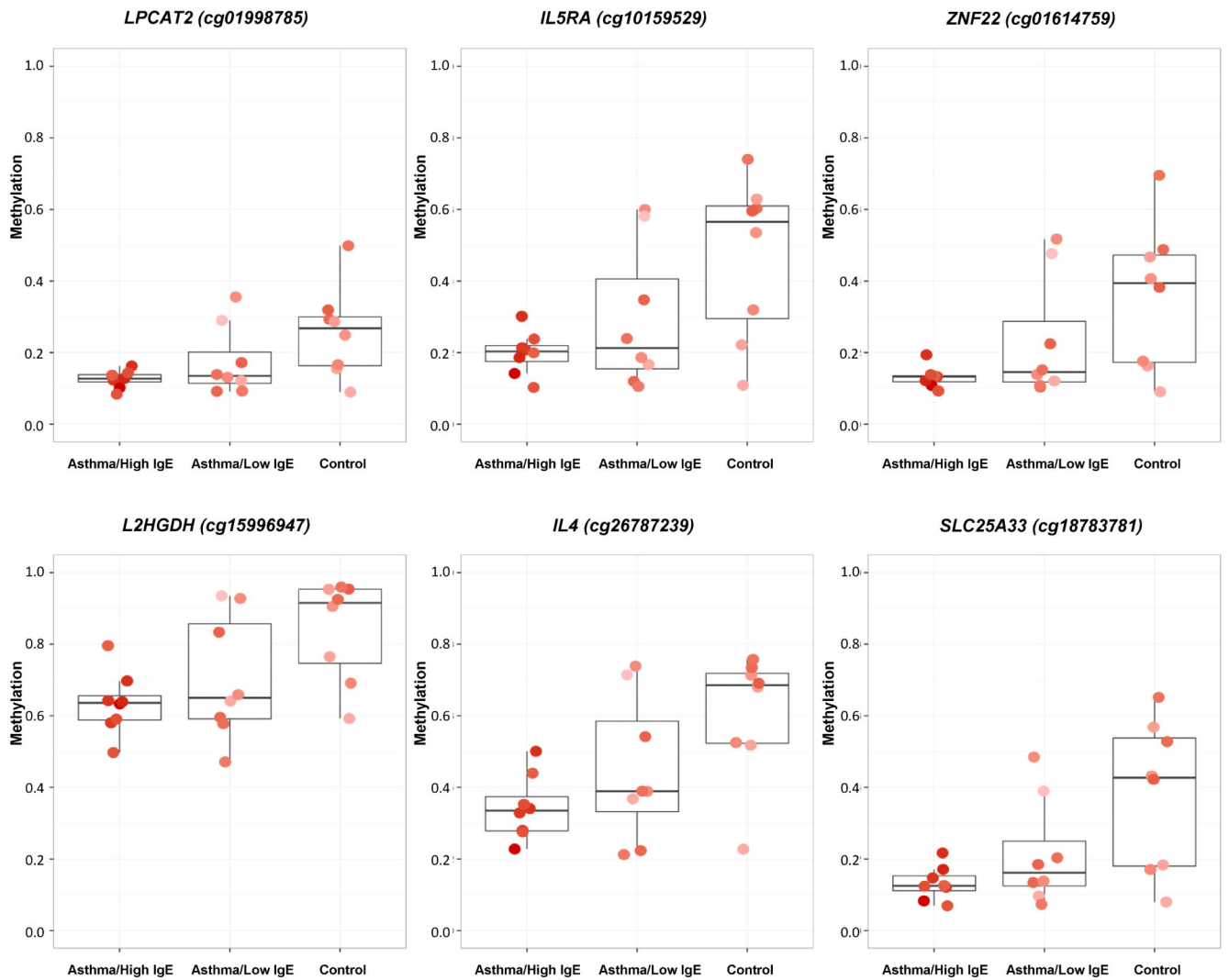


Figure 2. Boxplots of methylation at selected CpG loci in isolated eosinophils from subjects with and without asthma and high total serum IgE concentrations (>110 IU/l)
 Subjects were derived from the SLSJ population. Methylation (β) is shown on a scale of 0-1 for 8 subjects in each group. Boxplots show means and interquartile ranges. The intensity of the data point colour is proportion to total serum IgE. All loci exhibited reduced variability and levels of methylation in the subjects with asthma and high IgE ($P < 0.05$).

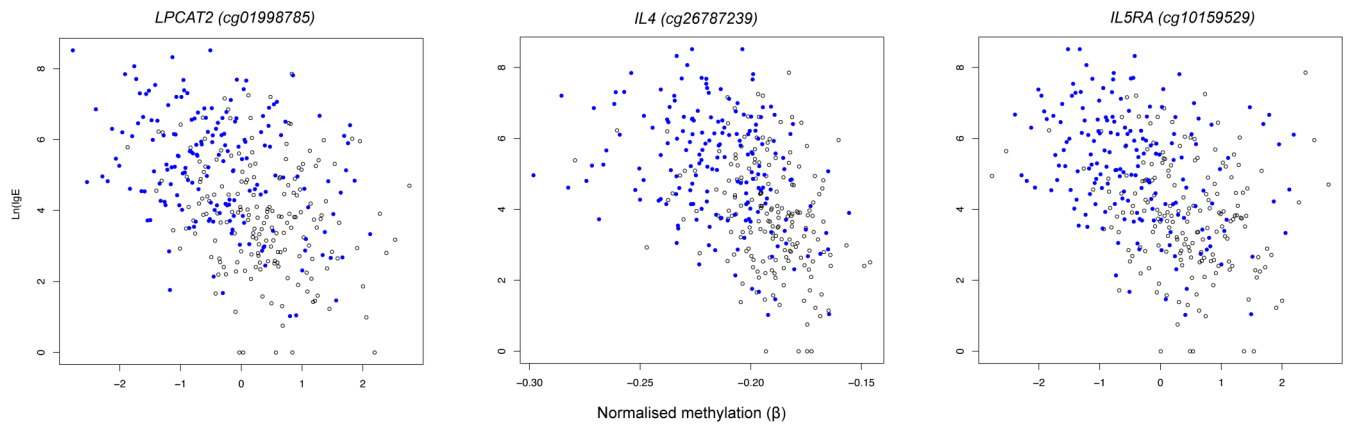


Figure 3. Association of selected CpG loci to total serum IgE concentrations in the MRCA panel, partitioned by eosinophil counts
Methylation values for 355 individuals normalised around a mean of 0 on the abscissa (x) with $\ln(\text{IgE})$ levels on the ordinate. Blue dots indicate subjects with eosinophil counts greater than the median for the MRCA panel.

Table 1
Subject characteristics

	MRCA (discovery)	PAPA (1st replication)	SLSJ (2nd replication)
Number	355	149	160
Age (Mean, range)	28, 2-61	21, 18-30	29, 5-79
N (%) Female	172 (48.5%)	72 (48.3%)	80 (50.0%)
N (%) Asthmatic	175 (49.3%)	34 (22.8%)	69 (43.1%)
N (%) Smokers	45 (12.7%)	33 (22.1%)	28 (17.5%)
Eosinophil count (mean \pm SE) per mcl *	406 \pm 383	246 \pm 214	242 \pm 205
Geometric Mean Serum IgE (Range) IU/L †	320, 1-4999	663, 0-18800	412, 2-7653

* Normal range <350 cells per mcl;

† Normal range <100 IU/L

Table 2
Meta-analysis of association of total serum IgE concentration in three subject panels

Probe	Symbol	Function	P MRCA	P SLSJ	P PAPA	P Meta
cg01998785	LPCAT2	Lysophospholipid metabolism	1.2E-13	8.0E-03	9.6E-06	1.2E-18
cg10159529	IL5RA	Cytokine signalling	5.1E-12	2.1E-04	7.2E-05	2.2E-18
cg01614759	ZNF22	Transcription Factor	4.4E-12	3.4E-03	2.8E-06	2.8E-18
cg15996947	L2HGDH	Mitochondrial oxidoreductase	7.4E-13	1.0E-02	3.7E-05	2.8E-17
cg26787239	IL4	Cytokine signalling	1.6E-11	1.3E-03	4.8E-04	3.2E-16
cg18783781	SLC25A33	Mitochondrial transport: dendritic cell endocytosis	5.0E-14	3.4E-02	6.2E-03	4.4E-15
cg13221796	RB1	Transcription Factor	5.7E-10	6.0E-02	4.9E-06	2.5E-14
cg01770400	SERPINC1	Anti-thrombin	6.6E-12	7.0E-03	1.3E-02	5.3E-14
cg02643667	TFF1	Mucus stabilising secreted protein	7.9E-12	1.3E-01	2.6E-03	7.6E-13
cg21627181	SLC17A4	Sodium/phosphate cotransporter	1.1E-06	1.4E-04	3.8E-04	1.1E-12
cg20189937	L2HGDH	Mitochondrial oxidoreductase	1.3E-06	2.4E-03	3.2E-05	2.6E-12
cg26457013	TMEM86B	Lysoplasmalogenase: phospholipid metabolism	1.0E-09	9.5E-02	9.0E-04	7.1E-12
cg20503329	COL15A1	Cell shape, motility, adhesion	1.2E-09	3.0E-01	8.8E-05	9.5E-12
cg03693099	CEL	Secreted carboxyl ester lipase	1.8E-08	1.1E-01	8.3E-05	1.3E-11
cg00079056	SPINK4	Serine peptidase inhibitor	1.5E-07	6.4E-02	3.1E-05	1.8E-11
cg09676390	ADARB1	Pre-mRNA editing of the glutamate receptor	1.2E-08	7.0E-02	8.0E-04	3.1E-11
cg15998761	MFSB6	MHC receptor homolog	9.3E-07	1.3E-02	1.7E-04	4.5E-11
cg25494227	TMEM52B	Transmembrane protein	1.3E-07	2.0E-01	1.2E-05	5.1E-11
cg11398517	FAM112A		2.4E-06	7.4E-03	3.3E-04	1.0E-10
cg06690548	SLC7A11	Cystine/glutamate antiporter: dendritic cell differentiation	2.7E-05	3.3E-04	1.1E-03	1.8E-10
cg17784922	KEL	Metallo-endopeptidase	4.2E-07	7.9E-03	4.4E-03	2.1E-10
cg16050349	PIK3CB	Catalytic subunit for PI3Kbeta: activation of neutrophils	4.0E-05	1.7E-03	2.3E-04	3.2E-10
cg25636075	TMEM41A	Transmembrane protein	2.5E-04	5.1E-05	7.7E-04	3.9E-10
cg08404225	IL5RA	Cytokine signalling	2.3E-04	3.3E-03	8.4E-06	4.1E-10
cg09447105	PDE6H	Inhibitory subunit of cGMP phosphodiesterase	2.2E-07	1.3E-01	4.0E-04	5.3E-10
cg05215575	SEPT12	Cell shape, motility, adhesion	3.1E-07	2.1E-01	2.7E-04	1.2E-09
cg26136776	KLF1	Erythroid-specific transcription factor	3.3E-08	4.3E-01	6.6E-04	1.5E-09
cg17749520	ITGA2B	Platelet fibronectin receptor: role in coagulation	1.4E-06	2.5E-02	3.5E-03	1.8E-09
cg24459209	PRG3	Eosinophil major basic protein homolog	3.3E-06	2.9E-02	1.1E-03	1.8E-09
cg00002426	SLMAP	Sarcolemma associated protein	7.9E-05	8.3E-03	1.6E-04	2.4E-09
cg15357945	PRG2	Eosinophil granule major basic protein	2.2E-03	2.8E-05	5.8E-04	3.1E-09
cg17582777	EFNA3	Receptor protein-tyrosine kinase	1.1E-04	3.1E-02	8.2E-05	8.6E-09
cg19881895	SLC43A3	Transmembrane protein	7.5E-05	2.8E-03	6.7E-03	1.6E-08
cg18254848	CLC	Lysophospholipid metabolism	1.8E-05	4.4E-02	4.6E-03	4.5E-08
cg21631409	ALDH3B2	Enzyme or Kinase	2.3E-04	1.7E-02	1.2E-03	6.8E-08
cg00536175	GATA1	Eosinophil transcription factor	7.9E-08	4.0E-01	5.1E-02	1.4E-07

Loci with a false discovery rate for the meta-analysis $<10^{-4}$ are shown: a full list of significant associations is in Supplementary Table 1. Markers are identified through their Illumina IDs and the associated gene symbol is derived from the Illumina annotation updated through PubMed. Note that two probes from *IL5RA* and from *L2HGDH* are associated to IgE concentrations.